Hydrol. Earth Syst. Sci. Discuss., 12, 9393–9436, 2015
www.hydrol-earth-syst-sci-discuss.net/12/9393/2015/
doi:10.5194/hessd-12-9393-2015


Hydrology and Earth System Sciences
Open Access
Discussions



# Simulating hydrology with an isotopic land surface model in western Siberia: what do we learn from water isotopes?

**F. Guglielmo[1], C. Risi[2], C. Ottlé[1], V. Valdayskikh[3], T. Radchenko[3], O. Nekrasova[3], O. Cattani[1], O. Stukova[3], J. Jouzel[1], V. Zakharov[3], S. Dantec-Nédélec[1], and J. Ogée[4]**

[1]Laboratoire des Sciences du Climat, Institut Pierre-Simon Laplace, CEA-CNRS-UVSQ, Gif-sur-Yvette, France
[2]Laboratoire de Météorologie Dynamique, Institut Pierre-Simon Laplace, Paris, France
[3]Ural Federal University, Yekaterinburg, Russian Federation
[4]INRA, UMR 1391 ISPA, 33140 Villenave d'Ornon, France

Received: 9 June 2015 – Accepted: 27 July 2015 – Published: 17 September 2015

Correspondence to: F. Guglielmo (francesca.guglielmo@lsce.ipsl.fr)

Published by Copernicus Publications on behalf of the European Geosciences Union.







## Abstract

Improvements in the evaluation of land surface models would translate into more reliable predictions of future climate changes, as significant uncertainties persist in the quantification and representation of the relative contributions of soil and vegetation to the water and energy cycles. In this paper, we investigate the usefulness of water stable isotopes in land surface models studying land surface processes. To achieve this, we implemented $^{18}O$ and $^{2}H$ and the computation of the oxygen ($\delta^{18}O$) and deuterium ($\delta D$) stable isotope composition of soil and leaf water pools in a recent version of the land surface model ORCHIDEE. We performed point-wise simulations with this new model and evaluated its performance on vertical profiles of soil water isotope ratios measured in summer 2012 at four experimental sites located in a boreal region of the Artic zone of western Siberia. The model performed relatively well in simulating some features of the $\delta^{18}O$ soil profiles, but poorly reproduced the d-excess profiles, at all four stations.

The response of the simulated $\delta^{18}O$ profiles to variations in key hydrological parameters revealed the importance of the choice of a correct infiltration pathway in ORCHIDEE. Our results show also that the strength of the evaporative enrichment signal plays a role in shaping the profiles, too and, therefore, the relevance of the vegetation and bare soil characterization. We investigated furthermore to which extent we are able to determine the relative contribution of the evaporation to the evapotranspiration.

This study's results confirm that the use of water stable isotopes measurements helps constrain the representation of key land surface processes in land surface models.





HESSD

12, 9393–9436, 2015



## 1 Introduction

Uncertainties in the representation of land surface processes in the land surface component of climate models may contribute significantly to the spread in climate projections (Pitman et al., 2009; Boé and Terray, 2008; Crossley et al., 2000). Several studies investigated in land surface models, both in stand-alone mode or coupled to atmospheric General Circulation Models (GCMs), the impact of key parameters on the soil hydrology and found that the contribution of the terrestrial biosphere to the water cycle was highly uncertain (Cheruy et al., 2013; Koster et al., 2006; Polcher, 1996). Improvements in the evaluation of such models would translate into more reliable predictions of future changes.

Water molecules carry hydrogen and oxygen isotopes in different proportions. The most common and stable species are hydrogen $^{1}H$ and oxygen $^{16}O$, yet heavier isotopologues, notably deuterium D and oxygen $^{18}O$, also occur as in HDO and $H_2^{18}O$, respectively. From a mere energetic point of view, this translates, at phase transitions, into preferential evaporation of the lighter isotopes (Daansgard, 1964). The extent of this fractionation is a function of the environmental conditions among which the temperature plays a key role. The fact that the isotopic composition of water is affected by phase changes makes it a reliable tracer for the hydrological cycle. Water stable isotopes have been used to investigate atmospheric processes (Worden et al., 2007; Gat et al., 2000). If the focus is the assessment of land surface processes, particularly relevant is the fact that soil evaporation and plant transpiration bear very distinct isotopic signatures (Mathieu and Bariac, 1996; Barnes and Allison, 1988). Water isotopic measurement could thus also be employed in the evaluation of the land surface hydrological budget (Williams et al., 2004; Moreira et al., 1997), of water recycling through land-surface evaporation, or to study vegetation transpiration (McGuffie and Henderson-Sellers, 2004; Pierrehumbert, 1999; Gat and Matsui, 1991; Salati et al., 1979).





HESSD
12, 9393–9436, 2015



Our main objective is here to confirm the usefulness of water isotopes in investigating land surface processes. Using similar approaches as in other isotope-enabled land surface models (Haese et al., 2013; Aleinov and Schmidt, 2006; Yoshimura et al., 2006; Cuntz et al., 2003), we implemented for this study water isotopes in the most recent version of the land surface model ORCHIDEE (following Risi, 2009), hereafter referred to as ORCHIDEE-iso.

Due to its unique hydrological features (presence of wetlands, permafrost), Siberia has been in recent years the focus of several climate change studies (e.g. Bulygina et al., 2015, 2011). In particular, studies focus on the sensitivity of Siberian hydrological and biogeochemical cycles to climate perturbations, especially in view of a warming trend (e.g. Walter et al., 2006). Of particular concern is a possible deepening of the soil seasonal melting layer, the Active Layer Thickness, which could bear effects on the hydrological cycle as well as on the greenhouse gas budget, considering the large amount of carbon stored in deep permafrost (Callaghan et al., 2011).

Being able to predict water oxygen isotopes in soil and leaf water pools is also a prerequisite to understand the global atmospheric budget of $CO^{18}O$, an atmospheric tracer used to disentangle land photosynthesis and respiration at large scale (Welp et al., 2011; Cuntz et al., 2003; Peylin et al., 1999). Because of its high continentality and strong seasonality, the Siberian plateau is amongst the regions of the world where the $CO^{18}O$ budget is the most informative on the land–atmosphere $CO_2$ fluxes (Wingate et al., 2009; Peylin et al., 1999), provided that the oxygen isotopes in soil and leaf water pools are well characterized.

In this study we thoroughly tested ORCHIDEE-iso's performance at instrumented stations located in a boreal region of Western Siberia on the left bank of the river Ob and investigated the added value of water isotopes in constraining the description of key hydrological processes in the model. For this, ORCHIDEE-iso stand-alone (i.e. not coupled to an atmospheric model) was set up and run at these four locations. The results of the simulations were evaluated against local vertical profiles of water isotopes in soil water.





HESSD
12, 9393–9436, 2015



## 2 Methodology

### 2.1 Isotope basics

As hydrogen and oxygen stable isotopes in water molecules are closely associated, isotopic ratios and fractionations of the two elements are usually discussed together. In this study, following common practice, we refer to the isotopic enrichment by the $\delta$-notation relative to the Vienna Standard Mean Ocean Water (VSMOW, Coplen, 1996):

$$\delta = \left( \frac{R_{\text{sample}}}{R_{\text{VSMOW}}} - 1 \right) \cdot 1000 \quad (1)$$

$R_{\text{sample}}$ and $R_{\text{VSMOW}}$ are here the molar ratios of heavy to light water isotopes of the sample pool and of the reference ocean water, respectively. We have $R_{\text{VSMOW}} = 0.0020052$ for $^{18}O/^{16}O$ and 0.00015576 for D/H.

Expressed in ‰, $\delta$D and $\delta^{18}$O denote the enrichment of a sample in HDO and $H_2^{18}O$, respectively. Based on precipitation collected from locations around the globe, Craig (1961) observed that $\delta^{18}$O and $\delta$D in freshwaters and precipitation that has not yet evaporated, follow the linear relation:

$$\delta D = 8 \cdot \delta^{18}O + 10 \quad (2)$$

the Global Meteoric Water Line (GMWL). Deuterium excess is thus defined as:

$$\text{d-excess} = \delta D - \delta^{18}O + 10 \quad (3)$$

Local deviations from the GMWL correspond to deviations from Rayleigh equilibrium condensation (Craig, 1961). The study of d-excess in precipitation can thus help infer the environmental conditions triggering non-equilibrium processes all along the path of the air masses from source areas to the regions where precipitation occurs (Merlivat and Jouzel, 1979).





HESSD
12, 9393–9436, 2015



## 2.2 Observation data

Vertical profiles of $\delta^{18}O$ and $\delta D$ in soil moisture, were measured in August 2012 at four locations at the Labytnangi Ecological Research Station (66°39′34.5″ N, 66°24′31.9″ E). The territory, located at the western edge of West Siberian Plain on the left bank of the river Ob, is generally characterized by poorly drained soils creating floodplains and swamps and presents a certain spatial variability in geology, vegetation cover and soil particle size distribution, but no significant relief. The height a.s.l. varies between 90 and 110 m. The local climate is characterized by cold winters (average annual temperature is −7.1 °C), low precipitation rates (average total annual precipitation is around 400, 220 mm of which is snow), snow cover from October to May (average 32.4 mm), and a short plant growing season (Valdayskikh et al., 2013).

The measurement stations, delimiting a triangular 30 $km^2$ area (Fig. 1), span each over 1 $km^2$; they have been selected and mapped (Valdayskikh et al., 2013) to give a picture as thorough as possible of the heterogeneity of the territory. Here we summarize their main features that are of significance for our study. Based on vegetation communities, three main ecosystems are observable: tundra (stations 1 and 2), peat bog (station 3), and floodplain (station 4). Moreover, at least two hydrological regimes (swamp, alluvial plain) are identifiable. The two tundra sites, both located on the left native shore of the river Ob, differ in soil texture, with station 1 showing silty loam soils and station 2 having coarse textured soils (sandy loam). The vegetation cover is spatially inhomogeneous showing shrubs, mosses, lichens as well as dwarf birches (these latter mostly at station 1). The peat soil of the swamp site (station 3) presents a relevant clay fraction. Station 4, the closest to the riverbank, is an alluvial floodplain with fine (silty) soils. The flooded state of such site during the measurement campaign (the latter having been nevertheless successful) prevents from a detailed characterization of its vegetation coverage.

The heterogeneity of the study area in Labytnangi is reflected in the depth of the permafrost. The shallowest seasonal melting layer is found for station 3 at 40 cm, the





HESSD
12, 9393–9436, 2015



peat surface layers ensuring good thermal insulation. Station 2, on the other hand, shows the highest heat conductivity. The seasonal melting layer is at this site much deeper, being located at 125 cm. For the finer soils of the other tundra site (station 1), the conductivity gradient is less pronounced and the permafrost starts at 70 cm.

At each site, three soil cores were collected and divided into 10 cm sections. The water was then extracted from the soil samples by vacuum distillation. A laser-based water analyzer (L2130-I, Picarro Inc., Santa Clara, USA), installed at the Climate and Environmental Physics Laboratory of the Ural Federal University (Yekaterinburg, Russian Federation), was used to determine the $\delta^{18}O$ and $\delta D$ of the extracted water samples. Instrumental precision is 0.4 ‰ for deuterium and 0.05 ‰ for $^{18}O$. The instrument calibration was carried out using three reference water standards (DW1 – distilled water, YEKA1 – Antarctic snow and distilled water mix, DOMEC – Antarctic snow).

### 2.3 Model description

ORCHIDEE-iso (Risi, 2009) is based on the land surface model ORCHIDEE (Krinner et al., 2005) developed at the Institut Pierre-Simon Laplace (IPSL), in France. The setup used for this study is the natural evolution of the one developed and extensively tested by Risi (2009) and has been accordingly evaluated against isotopic water measurement at stations, representative of different climates, belonging to the MIBA (Moisture Isotopes in Biosphere and Atmosphere) network (Wingate et al., 2010; Raz-Yaseef et al., 2010; Knohl et al., 2007). Differences between the two ORCHIDEE-iso setups solely depend on differences between the version of ORCHIDEE isotopes were originally implemented in and a more recent version of ORCHIDEE this study is based on.

ORCHIDEE includes three separate modules: SECHIBA resolves water and energy exchanges between land surface and atmosphere (de Rosnay, 1999; Ducoudré et al., 1993); STOMATE accounts for vegetation phenology and growth and for the carbon cycle (Krinner et al., 2005); LPJ (Sitch, 2003) simulates the dynamic evolution





HESSD
12, 9393–9436, 2015



of the vegetation cover through competition and fire. The model considers different land cover types in boreal, temperate, and tropical regions: within each grid cell bare soil, deciduous or evergreen forests, C3 and C4 grasslands may co-exist, up to a maximum of 12 different plant functional types (characterized by leaf area index, albedo, root depth, height, among others), for which water fluxes and reservoirs are computed independently. In this study the STOMATE and LPJ modules were not activated; prescribed land cover maps and related parameters were used instead, with vegetation phenology parameterized according to a simple growing degree day (GDD) model.

ORCHIDEE can run at different spatial scales, from point-wise simulations up to global experiments. The standard temporal resolution is of 30 min. The model represents all fluxes and pools relevant for the soil water budget. Throughfall rain, snowmelt and throughfall dew reach the soil surface. In the ORCHIDEE setup (Choisnel et al., 1995) used for this study the soil is 2 m deep and contains a superficial and a bottom water reservoir. When the water content exceeds the total soil holding capacity (300 mm), runoff occurs, partitioned into 95 % drainage and 5 % surface runoff (Ngo-Duc, 2005). Snow is represented by a single layer reservoir subject to melting and sublimation. ORCHIDEE resolves different fluxes contributing to the evapotranspiration: bare soil evaporation, vegetation transpiration (soil-moisture-limited), and evaporation of water intercepted by the vegetation canopy.

Water stable isotopes $^{18}O$ and $^{2}H$ were implemented in the SECHIBA module, in parallel to the soil water ($^{1}H_{2}^{16}O$) cycle (Fig. 2). Fluxes in liquid phase in and out of the soil were assumed to occur without isotopic fractionation; surface runoff carries thus the $\delta^{18}O$ and $\delta D$ signals of the source flux (precipitation or snowmelt) and drainage has the isotope composition of the soil water it originates from. Isotope fractionation processes during snow sublimation or plant transpiration were neglected and plant transpiration was assumed to carry the isotope signature of its source (soil) water (Barnes and Allison, 1988; Washburn and Smith, 1934). As SECHIBA does not account for water vapor transport in soils, fractionation during water vapor diffusion in the soil column (Melayah et al., 1996) could not be implemented. Isotope fractionation occurs solely





HESSD
12, 9393–9436, 2015



during evaporation of bare soil or of liquid water intercepted by the canopy (Craig and Gordon, 1965).

In spite of the unresolved vertical dimension of soil water pool of the ORCHIDEE setup it is based on, we endowed ORCHIDEE-iso with a diagnostic representation of the vertical distribution of water stable isotopes in the soil column. The approach, originally implemented by Risi (2009) ensures water budget conservation along the total soil column (and thus it does not interfere with the soil water budget of ORCHIDEE). Soil water is vertically distributed over several layers, defined, based on the available water soil water, from the top to the bottom of the soil column. At each time step, water sources and sinks are budgeted and, if necessary, the discretization revised; the isotopic composition is updated accordingly. The uppermost layer contains the water pool subject to bare-soil evaporation and has a water equivalent height:

$$L = \sqrt{K_{\mathrm{D}} \cdot dt} \tag{4}$$

$L$, a function of the effective self-diffusivity of liquid water in soil $K_{\mathrm{D}}$, is here the average distance traveled by water molecules in soil at each time-step $dt$. Further layers are created with fixed thickness, and progressively totally filled with the available water until the deepest layer that may, therefore, not be full and is used to estimate the isotopic composition of drainage. The composition of transpiration is calculated as the average composition of soil water along the soil column, weighted by the root extraction profile used to calculate the sensitivity of transpiration to soil moisture (de Rosnay and Polcher, 1998). Based on the chosen infiltration pathway (see Sect. 3.3.2), precipitation is either added to the top layer (piston flow) or evenly distributed along the soil column (preferential pathways flow). Isotopic diffusion between two adjacent layers is also taken into account. In ORCHIDEE-iso, the effective self-diffusivity of liquid water in the soil is calculated as (Braud et al., 2005):

$$K_{\mathrm{D}} = D_{\mathrm{m}} \cdot \theta_{\mathrm{l}} \cdot \tau \tag{5}$$





HESSD
12, 9393–9436, 2015



where $D_m$ [$m^2 s^{-1}$] is here the molecular self-diffusivity of water, $\theta_l$ [unitless] is the volumetric content of liquid water and $g\tau$ [unitless] is the soil tortuosity. Independently of the temperature, the value attributed to $D_m$ is $2.5 \times 10^{-9}$ $m^2 s^{-1}$ for all isotopes considered (Harris and Woolf, 1980). Braud et al. (2005) suggest for the product $\theta_l \tau$ the value 0.1. The value of $L$ (Eq. 4) corresponding to the time step used in this study, 30 min, is then of about 0.7 mm. This is consistent with a value of 0.67 for $\tau$ (e.g. Braud et al., 2005) and with an average of about 15 % for $\theta_l$. As values for these parameters are difficult to constrain observationally and strongly varying in time and space, we investigate in the following the sensitivity of the soil moisture vertical profiles to different values of $\theta_l \tau$. Vapor diffusion in soil and possible associated fractionation are not considered (Melayah et al., 1996).

### 2.4 Numerical experiments

In this study ORCHIDEE-iso was run in stand-alone mode, point-wise, at four stations in Labytnangi (cf. 2.2) using ORCHIDEE's standard time resolution.

The model spin-up consisted in running ORCHIDEE iteratively five times over the same meteorological year (2012), at each location. A further year of simulation was then performed using initial state variable values from the spin-up simulations at each location.

In the following, we describe the meteorological forcing, the isotopic forcing, and the characterization of the stations in ORCHIDEE-iso based on the available soil and vegetation data at the measurement sites.

#### 2.4.1 Meteorological forcing

ORCHIDEE-iso was forced for all experiments by 6 hourly time series of locally-measured surface air temperature and humidity, wind speed, precipitation, shortwave and longwave downward radiation. All these meteorological fields, except precipitation and radiation, are routinely recorded at the WMO meteorological station of Salekhard,





HESSD
12, 9393–9436, 2015



20 km southeast of Labytnangi. For the missing variables, ERA-INTERIM reanalysis were used to complete the dataset. Due to the spatial proximity ($\leq$ 10 km) of the stations and to the absence of significant orographic features, we assumed that the meteorological conditions (advection of air masses, frequency, intensity, amount of the precipitation) did not significantly differ from site to site.

### 2.4.2 Isotopic forcing

Besides pure meteorological forcing, ORCHIDEE-iso requires the isotope composition of precipitation and water vapor as additional input variables as the relative composition of all land surface water reservoirs is, at the first order, driven by the composition of precipitation.

The $\delta$D and $\delta^{18}$O of rain were provided, for all stations, by a combination of measurements (monthly values) at Amderma, a station belonging to the International Atomic Energy Agency's Global Network for Isotopes in Precipitation (GNIP, Rozanski et al., 1993) and at two other stations, Tobolsk and Turuhalsk, from the Siberian Network for Isotopes in Precipitation (SNIP, Kurita et al., 2004). Given the distance of these different GNIP/SNIP stations from our study area (360 km north-west, 970 km south and 980 km east of Labytnangi, respectively), we further spatially interpolated the $\delta$D and $\delta^{18}$O values at the different stations to the study area assuming the same spatial patterns as those obtained by an isotopic simulation of the isotope-enabled atmospheric GCM LMDZ-iso (Risi et al., 2010). The isotopic composition of water vapor was calculated by adding to the composition of precipitation the difference between the composition in vapor and in precipitation simulated by LMDZ-iso (Risi et al., 2009).

### 2.4.3 Characterization of the stations

The four experimental stations were characterized in ORCHIDEE-iso by attributing different types of soil and plant functional types (Table 1). At this stage in the model it is not possible to represent more than one soil type at a time in each grid cell and





HESSD
12, 9393–9436, 2015



for the whole soil column. The soils were thus classified according to the predominant grain size (sand, silt or clay, as defined by USDA, the United States Department of Agriculture) at each station, using data collected in summer 2012 by the University of Yekaterinburg (Valdayskikh et al., 2013, and summarized in Sect. 2.2).

Plant function types were characterized by a predominance of C3 grass at all stations, with a maximum fraction, 99 %, at station 3. Boreal broad-leaf summer-green trees were, although in different, limited proportions, represented at all sites. Station 1 and 2, located in the tundra, also host deciduous needleleaf species (*Larix*). Station 4 was flooded during the study period, but differs from station 3 only by having 30 % of bare soil (Table 1), an assumption somewhat arbitrary, but that could be evaluated by comparing results from these two stations. Moreover, a higher percentage of bare soil for this site, when direct information is not present, is indirectly inferable from the experimental profiles analyzed in the following.

## 3 Results

In this section we first present the experimental soil water isotope profiles and then we proceed in evaluating the ability of ORCHIDEE-iso to reproduce $\delta^{18}O$ and d-excess, after the tuning of some physical or hydrological parameters. Once analyzed the best fitting simulation for each site, we show the sensitivity of the isotopic profiles to variations in those parameters. We calculate the contributions of different vegetation covers and soil properties in shaping the $\delta^{18}O$ profiles between the different sites. Finally, we examine the potentialities of water isotopes in constraining, in ORCHIDEE-iso, a term of the water budget, namely the evaporation with respect to the evapotranspiration.





HESSD
12, 9393–9436, 2015



### 3.1 Observation data analysis

For each station, three profiles of $\delta^{18}O$ and $\delta D$ in soil moisture, down to a maximum depth of 1 m, were measured at different locations within an area of 1 $km^2$ so as to take into account the spatial variability characterizing each station. The depth of the profiles differed among the stations; when less than 1 m, it was imposed by the presence of permafrost, which inhibited the sampling activity below. For all profiles of all stations, the standard deviation associated to the measuring uncertainty $\sigma_m$ is $\approx 0.3$ ‰ and $\approx 3$ ‰ for $\delta^{18}O$ and $\delta D$, respectively (not shown). At each station we calculated an average profile of $\delta^{18}O$ and d-excess and estimated the intra-site spatial variability.

We assume that meteorological conditions do not significantly differ from station to station and that, therefore, differences in isotopic enrichment among the sites mostly arose from different characteristic of the soils and of the vegetation cover. At short temporal scales, it cannot be nevertheless excluded that episodic weather phenomena influenced differently the stations far from one another.

#### 3.1.1 $\delta^{18}O$

We show the average profiles of $\delta^{18}O$ in Fig. 3 (brown curves) with the associated dispersion $\sigma_s$, expressing the intra-site spatial variability; its high magnitude is a direct consequence of the heterogeneity of the territory.

All profiles of Fig. 3 show an isotopic enrichment near the surface. This is due to the preferred evaporation of the lighter isotopes from bare soil (Barnes and Allison, 1998). At the surface (first 10 cm), the highest isotopic enrichment is shown at the alluvial plain (station 4). This is linked to the comparatively higher bare soil evaporation and justifies the choice of characterizing this site in ORCHIDEE-iso with explicit presence of bare soils (see Table 1), unlike the remaining three stations. Riverine waters originating elsewhere, in areas of more enriched precipitation, may have also contributed to the high surface values of this flooded site. The surface enrichment at the tundra stations





HESSD
12, 9393–9436, 2015



(1 and 2) does not seem to be influenced by differences in soil texture between the two sites.

Proceeding downwards, the $\delta^{18}O$ curves show the steepest vertical gradient at the peat-bog site (station 3), for which the enrichment drops by 3.5 ‰ within the first 20 cm. For this site, a thick sub-superficial peat layer (Valdayskikh et al., 2013) may have inhibited the vertical diffusion of water, leading to an isotopic enrichment confined to the first centimeters. In this case, the evaporative signal propagates downwards mostly with infiltration of surface water. The profiles at station 1 and station 4 show comparably smoother transitions, whereas soil water at station 2 is only 1 ‰ less enriched at 30 cm. In this latter case, depleted rainfall could have reached deeper because of the higher permeability of the sandy soil, especially in comparison to the other tundra site, station 1, having finer soils. Below 20 cm, station 1 and 3 exhibit a secondary enrichment peak (+0.5 and +1 ‰, respectively) at 40 cm. For both stations this local maximum recedes completely within the following 10 cm. The shape of the curves for station 1 and 3 mirrors their seasonal history. Rainfall is more depleted in winter and more enriched in summer (Gryazin et al., 2014); we observe therefore in the warm season more enriched soil water. At station 2, on the other hand, we do not observe any peak and the enrichment diminishes until the end of the profile showing its sharpest gradient (−1 ‰) between 20 and 40 cm. The known higher permeability of the soil at this site could have mixed the signals, obliterating the secondary (summer) maximum. At the flooded site (station 4), between 20 and 100 cm the vertical gradients smoothen significantly and the enrichment only diminishes by −0.5 ‰. No significant changes in the concavity are to be seen anywhere along the profile, i.e. station 4 does not seem to bear any memory of its seasonal history.

### 3.1.2 d-excess

In Fig. 4 we show d-excess profiles calculated from observed $\delta D$ and $\delta^{18}O$ in soil water (red curves). As in the case of the $\delta^{18}O$ profiles of Fig. 3, the error shown





HESSD
12, 9393–9436, 2015



(orange areas) depicts the standard deviation associated to the relatively large small-scale intra-site spatial variability.

All profiles show a minimum near the surface. This descends from the fact that evaporation of HDO is favored during bare soil evaporation compared to evaporation of $H_2^{18}O$, in a proportion greater than eight-folds. This is due to kinetic effects (Twining et al., 2006). The curves at station 1 and 3 exhibit a strong seasonality with sharp gradients, anti-correlated with the ones of the corresponding $\delta^{18}O$ profiles. Winter maxima of d-excess have been observed in the GNIP network for the Northern Hemisphere (Kurita et al., 2004; Froehlich et al., 2002). At station 2 and 4 we observe rather smooth curves; the lack of a significant winter signal here reinforces the hypothesis of soil hydrology playing an active role in shaping the profiles, i.e. diluting the isotopic signatures so clear at other locations.

### 3.2 Model evaluation against measurements

The territory of Labytnangi, extremely heterogeneous in its vegetation cover, is characterized by marked horizontal and vertical variability in morphology, soil, and processes. The horizontal inter-site variability has been addressed by repeating the model tuning (below) for each of the study sites. The vertical heterogeneity in soil types at a given station is, on the other hand, not accounted for in ORCHIDEE at this stage, nor are vertical processes as cryoturbation (e.g. Bockheim and Tarnocai, 1998) that may alter the physical properties of the soil (e.g. in gley tundra) and/or determine rearrangements of the soil vertical structure, in turn affecting the isotopic composition of soil moisture.

With the goal of reproducing the observed vertical isotopic profiles, we investigated the sensitivity of the model output to various parameters influencing the infiltration, the bare-soil evaporation, and the vertical diffusion. Once identified the value of each parameter leading to the best fit to the observed profiles for each station, we checked its consistency both with the a priori knowledge of the sites (Valdayskikh et al., 2013) and with the information from the analysis of the observed isotopic profiles. In Fig. 3





HESSD
12, 9393–9436, 2015



and Fig. 4 (green curves) we show the outcome of the best simulation (i.e. the profiles closest to the observed values) of $\delta^{18}O$ and d-excess, respectively, at each station. The corresponding values for the tunable parameters are indicated in Table 2.

### 3.2.1 Simulated and observed $\delta^{18}O$

Figure 3 shows the best-simulated $\delta^{18}O$ profiles. Simulated profiles at station 1 and 2 show peculiar sharp turns in alternating directions in their sub-superficial patterns. This could be an artifact deriving from the diagnostic vertical discretization. Neglecting this effect, we appreciate for station 1 a qualitatively reasonable match to the observations, whereas, in case of station 2, the experimental data appear to be comparatively less well reproduced by the model. The mismatch involves mainly surface enrichment and localization of maximum vertical gradient, the magnitude of which, about 2 ‰, is overestimated by the model by a factor of 2. Differences in surface characterization between the tundra sites (12 % of the total coverage as boreal summer green species) and stations 3 and 4 do not seem to influence significantly the surface enrichment signal.

For station 3, we observe a good match in the surface enrichment and in the transition down to 25 cm; below this depth, however, the model does not capture the further sinuosity of the measurements. All in all, the best agreement with the measurements is obtained for station 4.

The model is able to capture for each site the recent summer enrichment, but not the memory of the previous summer, i.e. the secondary peak we observe 45 cm below the ground at station 1 and 3 in the experimental data. Two hypotheses may explain this mismatch. First, the previous year's evaporation signal may have been, in reality, considerably stronger than that of the current year. The previous year' signal in the simulations only results from the spin-up period, which has been performed by repeating the meteorological forcing for the year 2012 and, therefore, does not represent realistic conditions. Second, ORCHIDEE-iso may overestimate vertical transport processes leading to an excessive smoothing of the profiles.





HESSD
12, 9393–9436, 2015



### 3.2.2 Simulated and observed d-excess

Figure 4 shows the simulated d-excess profiles obtained using for the same stations the same values of the key parameters that led to the best fit of $\delta^{18}O$ in Fig. 3. It appears that the best fits for $\delta^{18}O$ do not fit equally well the d-excess profiles. At station 2 the model matches the relatively smooth profile from 20 cm downwards, whereas for station 3 only the superficial gradient is, qualitatively, captured. For the remaining two sites, the mismatch is both qualitative and quantitative.

The d-excess forcing might be affected by a large error, due to (1) the large error affecting d-excess measurements (Kurita et al., 2004), (2) the errors affecting the d-excess simulation with LMDZ, used to interpolate the d-excess measurements. The difficulties for GCMs to predict d-excess in precipitation at spatial and temporal (seasonal) scale are well known (Mathieu et al., 2002; Yoshimura et al., 2006; Risi et al., 2010). Based on this systematic bias, we focus in the following on $\delta^{18}O$.

## 3.3 Sensitivity studies

Profiles of isotopes in soil moisture may show steep vertical gradients (our study, Wingate et al., 2009; Gazis and Geng, 2004), resulting from a combination of surface evaporation and small-scale vertical hydrological processes, such as vertical infiltration. Vertical processes are described in ORCHIDEE-iso in a rather simplified and idealized way as compared to state-of-the-art LSMs, but even in vertically resolved modeling approaches, where they are explicitly described (de Rosnay, 1999), infiltration processes are still difficult to simulate (de Rosnay et al., 2002). With the aim of evaluating such processes in ORCHIDEE-iso, we investigated the sensitivity of the simulated isotopic profiles to vertical diffusivity, infiltration pathway of the precipitation (Gazis and Geng, 2004), which feed back on the relative proportions of evapotranspiration, surface runoff, and drainage (Boone et al., 2010; Ducharne et al., 1998), and to surface evaporation.





HESSD
12, 9393–9436, 2015



For each set of tests we considered as reference run the best fit obtained for $\delta^{18}O$, in Fig. 3, with the combination of parameters values indicated in Table 1; we proceeded then varying once at a time the vertical diffusivity, the infiltration pathway, and the bare soil fraction (directly determining the surface evaporation), in order to isolate and assess the sensitivity of the isotopic profiles to each of these key parameters.

### 3.3.1 Sensitivity to vertical soil water diffusivity

In Fig. 5 we show for each station the profiles corresponding to the best fit and those obtained with different values of $\theta_l\tau$, the product of soil tortuosity and moisture content. The higher this product, the higher are the absolute values below the surface, i.e. the stronger is the propagation in depth of the surface enrichment signal. Whereas for both tundra sites (stations 1 and 2), the differences among the curves start around 15 cm of depth, profiles at the other two stations show their sensitivity to $\theta_l\tau$ right below the surface. The maximum spread is reached at 40 cm, and corresponds to the minimum values of $\delta^{18}O$ for station 1, and at around 20 cm at stations 2–4. Below this depth the vertical gradients smoothen as for all the latter three sites the infiltration follows a preferential pathway (see below). In three out of four cases, the best fit is reached adopting for $\theta_l\tau$ the value of 0.2, higher than the value suggested by Braud et al. (2005) and used in ORCHIDEE-iso standard configuration (Risi, 2009).

### 3.3.2 Sensitivity to water infiltration pathway

The extent to which water infiltrates in soil depends in first place on the soil hydraulic conductivity, a function of the soil texture (e.g. percentage of sand, silt and clay) and structure. The coarser the soils, the larger the pores, and the faster the vertical transfer. A variety of factors (flow through shrinkage cracks, passages created by roots and earthworms) may though, in finer soils, result in the formation of highly water-conductive pathways. This feature may drastically raise the overall infiltration rate of such soils, otherwise characteristically slow.





HESSD
12, 9393–9436, 2015



The mechanism of water progressively penetrating in the soil with time, or piston flow, has been described by some conceptual models (e.g. Green and Ampt, 1911). In ORCHIDEE-iso, this pathway is represented by having the rainfall collected in first place only by the model upper soil layer and, then, having it propagate vertically with time. Preferential pathway is, on the other hand, represented in our model by evenly distributing the precipitation input throughout the soil column (i.e. assuming instantaneous vertical flow).

Figure 6 shows the impact of the chosen infiltration pathway on the simulated $\delta^{18}O$ vertical profiles. At first glance, a piston-like vertical propagation leads to a clearer traceability of the signal seasonality, whereas whenever the rainfall follows a preferential pathway vertical gradients are smoother. The profiles affected the most by the choice of the infiltration pathway are at station 2. Already at 20 cm of depth, the curves for this site start spreading, to grow apart by 1.4 ‰ in the following 80 cm. The sensitivity of the profile at this station is enhanced by the coarser (sandy) soil.

The infiltration pathway does not appear to significantly influence the surface enrichment, apart from a slight effect (higher by 0.5 ‰ for the piston case) in case of station 3.

The infiltration pathway best fitting the observation profiles is of preferential flow type for all stations except station 1. Piston-flow reproduces best the profile at this station, as it is characterized by thinner soil. In case of station 3, for which the seasonal signal is clear in the observations (Fig. 3), the curve obtained with piston-like transfer does not capture properly the 40 cm secondary peak in the data. The best fit for this site was selected based on the closest match provided by a preferential flow in the first portion (until 25 cm of depth) of the profile.

### 3.3.3 Sensitivity to different bare-soil fractions

In our ORCHIDEE setup, each plant functional type is associated with a seasonally varying portion of bare soil. This variation is calculated monthly according to the





HESSD
12, 9393–9436, 2015



following equation:

$$\text{bare\_soil} = \text{bare\_soil-vegetmax} \cdot e^{-\text{LAI}\cdot\text{ext\_c}} \quad (6)$$

where vegetmax represents the seasonally varying maximum proportion of the grid cell, which could be covered by the plant functional type, and LAI is the corresponding leaf area index. The parameter ext_c is the associated extinction coefficient (d'Orgeval, 2006).

In Fig. 7 we explore the impact of varying ext_c, i.e. modifying the relative fraction of bare soil, on the isotopic profiles. Increasing ext_c leads to lower values of bare_soil. Reduced amount of evaporated water translates, in turn, into lower isotopic surface enrichment. It is important here to stress the fact that the four sites are not directly comparable, as they were a priori differently characterized in terms of vegetation cover in the model (only the two tundra stations share the same fractions of PFTs, Table 1), and that the different bare soil fractions tested here are relative to the PFTs of this initial characterization. For station 2–4, for which the infiltration follows a preferential pathway, the effect of ext_c is remarkable, particularly in the first 20 cm of the soil column; station 2 and 4 have such effect propagating deeper. Both profiles have been obtained with a value of $\theta_l \tau$ higher than for station 3. In case of station 1, the profile corresponding to the highest fraction of bare soil (blue curve), i.e. to the highest evaporation, shows the highest values and the steepest vertical. The difference in enrichment with the curves obtained with lower bare soil fractions at the depth of 1 m is comparable with the difference at the surface. This could imply that beyond a certain evaporation threshold a strong enrichment signal in summer might not be any longer fully compensated by the depleted signal of the cold season and that, therefore, the profile not only bears a clearer memory of the past seasons, but also experiences a net shift toward higher values. This effect however, as we only observe it for this station, is clearly also arising from the piston-like infiltration we discussed previously. For station 2, sharing the same vegetation as station 1, but having a coarser soil, there is no difference among the curves, nor any gradient appreciable below 20 cm, as the infiltration is more effective.





HESSD
12, 9393–9436, 2015



In this case the sensitivity to variation in the ext_c parameter is accentuated by the piston-flow infiltration.

### 3.3.4 Interpreting inter-sites differences

With the aim of explaining the differences among different sites, we chose two among the four experimental sites: station 1 (silty tundra) and 4 (floodplain). The corresponding profiles have contrasting shapes and are relatively well captured by the model. At these two sites the best fits have been obtained with different values of the three tunable parameters, namely infiltration pathway, bare soil fraction, and vegetation cover. We tried to decompose the difference between the simulated profiles into the single contribution of each of those three parameters.

Figure 8 shows the differences between $\delta^{18}O$ profiles at station 1 and 4 for observations (green curve) and for corresponding model best fits (blue curve) as well as the curves obtained changing one parameter at a time (Table 3), showing the step-wise transition between the two profiles. The blue curve expresses the combined effect of the different infiltration pathway, fractional bare soil per PFT, and vegetation coverage.

The difference in the experimental data profiles (green, with associated standard deviation in yellow) shows a higher enrichment (negative values) at the surface for station 4. ORCHIDEE-iso, although qualitatively capturing such enrichment (blue curve), overestimates it. In the model world such enrichment might be due to the higher fractional bare soil in the vegetation coverage (Table 1) prescribed for station 4. This effect overcompensates the lower ext_c value. Below 30 cm, the tundra profile is less steep than for the floodplain; this is due to its piston-flow infiltration. The floodplain shows a steeper vertical gradient arising from the preferential pathway infiltration (orange). We can conclude that for these two stations the most prominent role in shaping the differences between the profiles is played by the bare soil fraction and by the infiltration pathway.





HESSD
12, 9393–9436, 2015



### 3.3.5 Studying $E/(E+T)$

The previous section has highlighted the impact of the bare soil fraction on the surface enrichment. Here we investigate whether water isotope observations allow us to estimate the contribution of bare soil evaporation to the evapotranspiration (defined here as sum of bare soil evaporation and transpiration), i.e. the $E/(E+T)$ ratio, based on the results of the simulations performed and presented in this study and on the available measured data.

The measured soil isotopic composition $\delta^{18}$O results from the superposition of the two distinct signals of precipitation and evaporative enrichment. We try to isolate these two contributions at station 1, by showing in Fig. 9 (red lines) the difference between $\delta^{18}$O observed in surface soil water and in annual mean precipitation. When calculating this latter, to take into account the seasonality in soil water recharge, we weighted monthly mean values (forcing fields of 2.4.2) by the simulated monthly mean difference between precipitation and evapotranspiration. Different red lines correspond therefore to different $ET$ values obtained with different bare soil fraction (as in 3.3.3) in ORCHIDEE-iso. Analogously we show at the same station the difference of simulated $\delta^{18}$O in soil and $\delta^{18}$O precipitation (yellow, green and blue points) and the corresponding simulated $E/(E+T)$ from all different ORCHIDEE-iso experiments as in the sensitivity tests of 3.3, i.e. varying bare soil fraction, vertical diffusivity, and infiltration pathway. Each point corresponds to a different run. Points lying on the same (diagonal) fitting line are values obtained with, different bare soil fraction, but sharing the same value for the other two tuning parameters.

The $x$ axis values corresponding to the intersection between lines fitting model results and observation lines indicate realistic values of $E/(E+T)$. $E/(E+T)$ can be therefore estimated using $\delta^{18}$O in soil moisture with an uncertainty of about 20 %. This uncertainty sums up the effect of measurement uncertainty and intra-site heterogeneity and of uncertainties in the choice of diffusivity and infiltration pathway.





HESSD
12, 9393–9436, 2015



## 4 Conclusions

This paper shows the results of simulations of vertical profiles of $\delta^{18}O$ and d-excess in soil moisture performed with the isotope-enabled land surface model ORCHIDEE-iso on four instrumented sites located in Western Siberia, representative of different ecosystems and hydrological regimes. Model results have been compared with observed vertical profiles of $\delta^{18}O$ and d-excess that have, in spite of their geographical proximity, high spatial variability, consequence of the heterogeneous vegetation coverage and soil texture. They show the superposition of seasonality of precipitation, evaporative enrichment at the surface, and vertical hydrological processes in proportions that vary depending on the stations.

ORCHIDEE-iso has been tuned at each station with respect to bare soil cover, infiltration pathway, and vertical diffusivity; it reproduces qualitatively and quantitatively well the surface enrichment in observed vertical profiles of $\delta^{18}O$ in soil moisture, but does not capture the deeper signal of the previous summer. This calls for an analysis of the representation of vertical processes in ORCHIDEE-iso. To a reasonable match in $\delta^{18}O$ does not currently correspond a good representation of d-excess. Such poor performance is related to a higher uncertainty in modeling d-excess. It could also be related to our choice of the best-fit, which is based on the simulation of $\delta^{18}O$. Moreover, uncertainty is also associated with kinetic fractionation and with the neglect of vapor diffusion in soil pores.

Sensitivity tests on the impacts of vertical soil water diffusivity and infiltration on the isotopic vertical composition simulated by ORCHIDEE-iso show that the choice of the infiltration pathway is essential in determining the shape of the profile and most relevant among the two parameters. A piston-like flow does not affect the surface enrichment, but highlights the memory of the past season below 20 cm of depth. Besides processes related to hydrology and vertical dynamics of the soil column, the memory of the past seasons in the profiles is determined by the absolute strength of the evaporative signal.





HESSD
12, 9393–9436, 2015



Vegetation characterization and bare soil coverage in ORCHIDEE-iso is another high-impact factor in the isotopes vertical composition.

Our approach combining model results and observations allowed estimating the ratio $E/E+T$ using $\delta^{18}O$ in soil moisture with an uncertainty of 20 %. In order to ensure higher accuracy, the key processes of the soil vertical dynamics, diffusivity and infiltration pathway, need to be better constrained. Isotopes measurements will help evaluate the parameterization of these key processes furthermore in vertically resolved land surface models.

A model set up with a basic a priori knowledge of a site could deliver further information on the site itself. We confirmed that interactions between model and measurements is not unidirectional, but mutual. If on one hand isotopes help in best tuning the model, simulation results help in tracing back information about conditions and processes at the experimental sites.

## 5 Outlook

The approach followed in this study appears to be even more promising in view of the current developments of ORCHIDEE toward a version for high latitudes. On one hand the model is transitioning to a setup with eleven vertical layers (de Rosnay et al., 2002), on the other hand, in progress is also the description of the dynamics of permafrost and of its interaction with snow and vegetation (Gouttevin et al., 2012), coupled with a vertically resolved snow model (Wang et al., 2013). This higher resolution in processes would confer a much higher degree of realism to the simulations.

Furthermore, to simulate the water cycle in modern climate scenarios and, among other things, address persistent and systematic biases affecting the models (Meehl et al., 2007), running simulations coupling ORCHIDEE-iso with an atmospheric general circulation model (Risi et al., 2013, 2010b) would be valuable. Improvements in the description of the partitioning of evapotranspiration into evaporation and transpiration,





HESSD
12, 9393–9436, 2015



which could benefit from isotopic measurements, may moreover help in reducing the uncertainties in the land surface hydrological response to climate change.

The observation data used in this study were the minimum required to test a land surface model. Ideally, measurements in all water reservoirs (soil, precipitation, water vapor – in situ or remotely detected –, leaf and stem water) and time-series (a full seasonal cycle, at monthly scale) would be desirable. Moreover, co-located temperature and soil moisture profiles should be taken, accompanied by complete meteorological forcing, to capture the variability at small-scale.

*Acknowledgements.* This work was partly supported by the WSibIso project with a grant of Ministry of Education and Science of the Russian Federation under the contract No. 11.G34.31.0064. The authors are thankful to E. Rakov and V. Gryazin (Ural Federal University) for fruitful discussions.

## References

Barnes, C. and Allison, G.: Tracing of water movement in the unsaturated zone using stable isotopes of hydrogen and oxygen, J. Hydrol., 100, 143–176, 1988.

Bockheim, J. G. and Tarnocai, C.: Recognition of cryoturbation for classifying permafrost-affected soils, Geoderma, 81, 281–293, doi:10.1016/S0016-7061(97)00115-8, 1998.

Boé, J. and Terray, L.: Uncertainties in summer evapotranspiration changes over Europe and implications for regional climate change, Geophys. Res. Lett., 35, L05702, doi:10.1029/2007GL032417, 2008.

Boone, A., Xue, Y., Poccard-Leclerq, I., Feng, J., and deRosnay, P.: Evaluation of the WAMME model surface fluxes using results from the AMMA land-surface model intercomparison project, Clim. Dynam., 35, 127–142, doi:10.1007/s00382-009-0653-1, 2010.

Braud, I., Bariac, T., Gaudet, J. P., and Vauclin, M.: SiSPAT-Isotope, a coupled heat, water and stable isotope (HDO and $H_2^{18}O$) transport model for bare soil, Part I, Model description and first verifications, J. Hydrol., 309, 301–320, 2005.

Bulygina, O. N., Groisman, P. Y., Razuvaev, V. N., and Korshunova, N. N.: Changes in snow cover characteristics over Northern Eurasia since 1966, Environ. Res. Lett., 6, 045204, doi:10.1088/1748-9326/6/4/045204, 2011.





HESSD

12, 9393–9436, 2015



Bulygina, O. N., Arzhanova, N. M., and Groisman, P. Y.: Icing conditions over Northern Eurasia in changing climate, Environ. Res. Lett., 10, 025003, doi:10.1088/1748-9326/10/2/025003, 2015.
Callaghan, T. V., Johansson, M., Anisimov, O., Christiansen, H. H., Instanes, A., Romanovsky, N., Smith, S.: Chapter, 5: changing permafrost and its impacts, in: Snow, Water, Ice and Permafrost in the Arctic (SWIPA): Climate Change and the Cryosphere, Arctic Monitoring and Assessment Programme (AMAP), Oslo, Norway, xii, 538 pp., 2011.
Cheruy, F., Campoy, A., Dupont, J. C., Ducharne, A., Hourdin, F., Haeffelin, M., Chiriaco, M., and Idelkadi, A.: Combined influence of atmospheric physics and soil hydrology on the simulated meteorology at the SIRTA atmospheric observatory, Clim. Dynam., 40, 2251–2269, 2013.
Choisnel, E. M., Jourdain, S. V., and Jacquart, C. J.: Climatological evaluation of some fluxes of the surface energy and soil water balances over France, Ann. Geophys., 13, 666–674, doi:10.1007/s00585-995-0666-y, 1995.
Coplen, T.: Normalization of oxygen and hydrogen isotope data, Chem. Geol., 72, 293–297, 1988.
Craig, H.: Isotopic variations in meteoric waters, Science, 133, 1702–1703, 1961.
Craig, H. and Gordon, L. I.: Deuterium and oxygen-18 variations in the ocean and marine atmosphere, in: Stable Isotopes in Oceanographic Studies and Paleotemperatures, Spoleto: Consiglio Nazionale delle Ricerche, edited by: Tongiorgi, E., Laboratorio di Geologia Nucleare, Pisa, 1–122, availablehere:http://climate.colorado.edu/research/CG/CraigGordon1965_Noone_small3.pdf (last access: September 2015), 1965.
Crossley, J. F., Polcher, J., Cox, P. M., Gedney, N., and Planton, S.: Uncertainties linked to land-surface processes in climate change simulations, Clim. Dynam., 16, 949–961, 2000.
Cuntz, M., Ciais, P., Hoffmann, G., and Knorr, W.: A comprehensive global three-dimensional model of $\delta^{18}O$ in atmospheric $CO_2$, 1. Validation of surface processes, J. Geophys. Res., 108, 4527, doi:10.1029/2002JD00315, 2003.
Dansgaard, W.: Stable isotopes in precipitation, Tellus, 16, 436–468, 1964.
de Rosnay, P. and Polcher, J.: Modelling root water uptake in a complex land surface scheme coupled to a GCM, Hydrol. Earth Syst. Sci., 2, 239–255, doi:10.5194/hess-2-239-1998, 1998.
de Rosnay, P., Polcher, J., Bruen, M., and Laval, K.: Impact of a physically based soil water flow and soil-plant interaction representation for modeling large-scale land surface processes. J. Geophys. Res., 107, ACL 3-1–ACL 3-19, doi:10.1029/2001JD000634, 2002.





HESSD
12, 9393–9436, 2015



d'Orgeval, T.: Impact du changement climatique sur le cycle de l'eau en Afrique de l'Ouest: modélisation et incertitudes, Université Pierre et Marie Curie (Paris), Thèse de doctorat, Sciences de la Terre, Paris, 6, 2006.
Ducharne, A., Laval, K., Polcher, J.: Sensitivity of the hydrological cycle to the parameterization of soil hydrology in a GCM, Clim. Dynam., 14, 307–327, 1998.
Ducoudré, N. I., Laval, K., and Perrier, A.: SECHIBA, a new set of parameterizations of the hydrologic exchanges at the land–atmosphere interface within the LMD atmospheric general circulation model, J. Climate, 6, 248–273, 1993.
Froehlich, K., Gibson, J. J., and Aggarwal, P. K.: Deuterium excess in precipitation and its climatological significance, in: Study of Environmental Change Using Isotope Techniques, International Atomic Energy Agency, Vienna, Austria, United Nations Educational, Scientific and Cultural Organization, Paris, France, Japan Science and Technology Corporation (Japan), p. 541, October 2002, 54–66, International conference on study of environmental change using isotope techniques, 23–27 April 2001, Vienna, Austria, 54–66, 2002.
Gat, J.: Atmospheric water balance-the isotopic perspective, Hydrol. Process., 14, 1357–1369, 2000.
Gat, J. R. and Matsui, E.: Atmospheric water balance in the Amazon basin: an isotopic evapotranspiration model, J. Geophys. Res., 96, 13179–13188, 1991.
Gazis, C. and Geng, X.: A stable isotope study of soil water: evidence for mixing and preferential flow paths, Geoderma, 119, 97–111, 2004.
Gouttevin, I., Krinner, G., Ciais, P., Polcher, J., and Legout, C.: Multi-scale validation of a new soil freezing scheme for a land-surface model with physically-based hydrology, The Cryosphere, 6, 407–430, doi:10.5194/tc-6-407-2012, 2012.
Green, W. H. and Ampt, G.: Studies on soil physics, 1. the flow of air and water through soils, J. Agr. Sci., 4, 1–24, 1911.
Gryazin, V., Risi, C., Jouzel, J., Kurita, N., Worden, J., Frankenberg, C., Bastrikov, V., Gribanov, K., and Stukova, O.: To what extent could water isotopic measurements help us understand model biases in the water cycle over Western Siberia, Atmos. Chem. Phys., 14, 9807–9830, doi:10.5194/acp-14-9807-2014, 2014.
Harris, K. A. and Woolf, L. A.: Pressure and temperature dependence of the self diffusion coefficient of water and oxygen-18 water, J. Chem. Soc. Faraday T., 76, 377–385, 1980.





HESSD
12, 9393–9436, 2015



Haese, B., Werner, M., and Lohmann, G.: Stable water isotopes in the coupled atmosphere–land surface model ECHAM5-JSBACH, Geosci. Model Dev., 6, 1463–1480, doi:10.5194/gmd-6-1463-2013, 2013.

Koster, R. D., Sud, Y. C., Guo, Z., Dirmeyer, P. A., Bonan, G., Oleson, K. W., Chan, E., Verseghy, D., Cox, P., Davies, H., Kowalczyk, E., Gordon, C. T., Kanae, S., Lawrence, D., Liu, P., Mocko, D., Lu, C. H., Mitchell, K., Malyshev, S., McAvaney, B., Oki, T., Yamada, T., Pitman, A., Taylor, C. M., Vasic, R., and Xue, Y.: GLACE: The global land–atmosphere coupling experiment, Part I: Overview, J. Hydrometeorol., 7, 590–610, doi:10.1175/JHM510.1, 2006.

Knohl, A., Tu, K. P., Boukili, V., Brooks, P. D., Mambelli, S., Riley, W. J., and Dawson, T. E.: MIBA-US: temporal and spatial variation of water isotopes in terrestrial ecosystems across the United States, Eos Trans. AGU, 88, Fall Meet. Suppl., Abstract B12C-0388, 2007.

Krinner, G., Viovy, N., de Noblet-Ducoudré, N., Ogée, J., Polcher, J., Friedlingstein, P., Ciais, P., Sitch, S., and Prentice, I. C.: A dynamic global vegetation model for studies of the coupled atmosphere–biosphere system, Global Biogeochem. Cy., 19, GB1015, doi:10.1029/2003GB002199, 2005.

Kurita, N., Yoshida, N., Inoue, G., and Chayanova, E. A.: Modern isotope climatology of Russia: a first assessment, J. Geophys. Res., 109, D03102, doi:10.1029/2003JD003404, 2004.

Mathieu, R. and Bariac, T.: A numerical model for the simulation of stable isotope profiles in drying soils, J. Geophys. Res., 101, 12685–12696, 1996.

McGuffie, K. and Henderson-Sellers, A.: Stable water isotope characterization of human and natural impacts on land–atmosphere exchanges in the Amazon Basin, J. Geophys. Res., 109, D17104, doi:10.1029/2003JD004388, 2004.

Melayah, A., Bruckler, L., and Bariac, T.: Modeling the transport of water stable isotopes in unsaturated soils under natural conditions: 1. Theory, Water Resour. Res., 32, 2047–2054, doi:10.1029/96WR00674, 1996.

Merlivat, L. and Jouzel, J.: Global climatic interpretation of the deuterium-oxygen, 18 relationship for precipitation, J. Geophys. Res., 84, 5029–5033, 1979.

Moreira, M., Sternberg, L., Martinelli, L., Victoria, R., Barbosa, E., Bonates, C., and Nepstad, D.: Contribution of transpiration to forest ambient vapor based on isotopic measurements, Glob. Change Biol., 3, 439–450, 1997.





HESSD
12, 9393–9436, 2015



Ngo-Duc, T.: Modélisation des bilans hydrologiques continentaux: variabilité interannuelle et tendances, Comparaison aux observations, PhD Thesis, Université Pierre et Marie Curie, Paris VI, 2005.

Ogée, J., Cuntz, M., Peylin, P., and Bariac, T.: Non-steady-state, nonuniform transpiration rate and leaf anatomy effects on the progressive stable isotope enrichment of leaf water along monocot leaves, Plant Cell Environ., 30, 367–387, 2007.

Peylin, P., Ciais, P., Denning, S. A.,Tans, P. P., Berry, J. A., White, J. W. C.: A 3-dimensional study of $\delta^{18}O$ in atmospheric $CO_2$: contribution of different land ecosystems, Tellus B, 51, 642–667, doi:10.1034/j.1600-0889.1999.t01-2-00006.x, 1999.

Pitman, A. J., de Noblet-Ducoudré N., Cruz, F. T., Davin, E. L., Bonan, G. B., Brovkin, V., Claussen, M., Delire, C., Ganzeveld, L., Gayler, V., van den Hurk, B. J. J. M., Lawrence, P. J., van der Molen, M. K., Müller C., Reick, C. H., Seneviratne, S. I., Strengers, B. J., and Voldoire, A.: Uncertainties in climate responses to past land cover change: first results from the LUCID intercomparison study, Geophys. Res. Lett., 36, L14814, doi:10.1029/2009GL039076, 2009.

Pierrehumbert, R. T.: Huascaran $\delta^{18}O$ as an indicator of tropical climate during the Last Glacial Maximum, Geophys. Res. Lett., 26, 1345–1348, 1999.

Polcher, J., Laval, K., Dümenil, L., Lean, J., and Rowntree, P. R.: Comparing three land surface schemes used in general circulation models, J. Hydrol., 180, 373–394, 1996.

Raz-Yaseef, N., Yakir, D., Rotenberg, E., Schiller, G., and Cohen, S.: Ecohydrology of a semi-arid forest: partitioning among water balance components and its implications for predicted precipitation changes, Ecohydrology, 3, 143–154, 2010.

Risi, C.: Les isotopes stables de l'eau: applications à l'étude du cycle de l'eau et des variations du climat, Thèse de Doctorat, Université Pierre et Marie Curie, Paris VI, 2009.

Risi, C., Bony, S., Vimeux, F., and Jouzel, J.: Water-stable isotopes in the LMDZ4 general circulation model: Model evaluation for present-day and past climates and applications to climatic interpretations of tropical isotopic records, J. Geophys. Res., 115, D12118, doi:10.1029/2009JD013255, 2010a.

Risi, C., Bony, S., Vimeux, F., Frankenberg, C., Noone, D., and Worden, J.: Understanding the Sahelian water budget through the isotopic composition of water vapor and precipitation, J. Geophys. Res., 115, D24110, doi:10.1029/2010JD014690, 2010b.

Risi, C., Noone, D., Frankenberg, C., and Worden, J.: Role of continental recycling in intraseasonal variations of continental moisture as deduced from model simulations





HESSD
12, 9393–9436, 2015



and water vapor isotopic measurements, Water Resour. Res., 49, 4136–4156, doi:10.1002/wrcr.20312, 2013.
Rozanski, K., Araguás-Araguás, L., and Gonfiantini, R.: Isotopic patterns in modern global precipitation, in: Climate change in continental isotopic records, Geophys. Monogr. Ser., 78, AGU, Washington, DC, 1–36, 1993.
Salati, E., Dall'Olio, A., Matsui, E., and Gat, J.: Recycling of water in the Amazon basin: an isotopic study, Water Resour. Res., 15, 1250–1258, 1979.
Sitch, S., Smith, B., Prentice, I. C., Arneth, A., Bondeau, A., Cramer, W., Kaplan, J., Levis, S., Lucht, W., Sykes, M., Thonicke, K., and Venevski, S.: Evaluation of ecosystem dynamics, plant geography and terrestrial carbon cycling in the LPJ dynamic vegetation model, Glob. Change Biol., 9, 161–185, 2003.
Twining, J., Stone, D., Tadros, C., Henderson-Sellers, A., and Williams, A.: Moisture isotopes in the biosphere and atmosphere (MIBA) in Australia: a priori estimates and preliminary observations of stable water isotopes in soil, plant and vapour for the Tumbarumba field campaign, Global Planet. Change, 51, 59–72, doi:10.1016/j.gloplacha.2005.12.005, 2006.
Valdayskikh, V., Nekrasova, O., Jouzel, J., Uchaev, A., Radchenko, T.: Some characteristics of forest-tundra (West Siberia) soil groups distinguished on the basis of thermal properties, Prace Geograficzne, 135, 73–86, doi:10.4467/20833113PG.13.024.1552, 2013.
Walter, K. M., Zimov, S. A., Chanton, J. P., Verbyla, D., and Chapin III, F. S.: Methane bubbling from Siberian thaw lakes as a positive feedback to climate warming, Nature, 443, 71–75, doi:10.1038/nature05040, 2006.
Wang, T., Ottlé, C., Boone, A., Ciais, P., Brun, E., Morin, S., Krinner, G., Piao, S., and Peng, S.: Evaluation of an improved intermediate complexity snow scheme in the ORCHIDEE land surface model, J. Geophys. Res.-Atmos., 118, 6064–6079, doi:10.1002/jgrd.50395, 2013.
Washburn, E. and Smith, E.: The isotopic fractionation of water by physiological processes, Science, 79, 188–189, 1934.
Welp, L. R., Keeling, R. F., Meijer, H. A. J., Bollenbacher, A. F., Piper, S. C., Yoshimura, K., Francey, R. J., Allison, C. E., and Wahlen, M.: Interannual variability in the oxygen isotopes of atmospheric $CO_2$ driven by El Niño, Nature, 477, 579–582, doi:10.1038/nature10421, 2011.
Williams, D. G., Cable, W., Hultine, K., Hoedies, J. C. B., Yepez, E. A., Simonneaux, V., Er-Raki, S., Boulet, G., de Bruin, H. A. R., Chehbouni, A., Hartogensis, O. K., and Timouk, F.: Evapotranspiration components determined by stable isotope, sap flow and eddy covariance techniques, Agricult. Forest. Meteor., 934 125, 241–258, 2004.





HESSD
12, 9393–9436, 2015



Wingate, L., Ogée, J., Cuntz, M., Genty, B., Reiter, I., Seibt, U., Yakir, D., Maseyk, K., Pendall, E. G., Barbour, M. M., Mortazavi, B., Burlett, R., Peylin, P., Miller, J., Mencuccini, M., Shim, J. H., Hunt, J., and Grace, J.: The impact of soil microorganisms on the global budget of $\delta O^{18}$ in atmospheric $CO^2$, P. Natl. Acad. Sci. USA, 106, 22411–22415, doi:10.1073/pnas.0905210106, 2009.

Wingate, L., Ogée, J., Burlett, R., and Bosc, A.: Strong seasonal disequilibrium measured between the oxygen isotope signals of leaf and soil $CO_2$ exchange, Glob. Change Biol., 16, 3048–3064, doi:10.1111/j.1365-2486.2010.02186.x, 2010.

Worden, J., Noone, D., and Bowman, K.: Importance of rain evaporation and continental convection in the tropical water cycle, Nature, 445, 528–532, doi:10.1038/nature05508, 2007.

Yoshimura, K., Miyazaki, S., Kanae, S., and Oki, T.: Iso-MATSIRO, a land surface model that incorporates stable water isotopes, Global Planet Change, 51, 90–107, 2006.





HESSD
12, 9393–9436, 2015



**Table 1.** Bare soil, vegetation coverage (fraction of the grid cell), and soil type (predominant USDA grain size) in ORCHIDEE for the four simulation sites. Vegetation is expressed in terms of plant functional types.

| | station | bare soil | boreal broad-leaf summer-green | boreal needle-leaf summer-green1 | C3 grass | soil texture |
|---|---|---|---|---|---|---|
| tundra | 1 | 0 | 0.04 | 0.08 | 0.88 | silt |
| | 2 | 0 | 0.04 | 0.08 | 0.88 | sand |
| swamp | 3 | 0 | 0.01 | 0 | 0.99 | silt |
| floodplain | 4 | 0.3 | 0.01 | 0 | 0.69 | silt |





HESSD
12, 9393–9436, 2015



**Table 2.** Values of the tunable parameters for which the simulated profiles best fit the observations in $\delta^{18}O$ profiles. The infiltration pathway follows a piston-like or a preferential flow, the factor $\theta_l\tau$ contributes to the vertical diffusivity, and the extinction coefficient determines the fractional bare soil coverage for each given plant functional type.

| station | infiltration pathway | $\theta_l\tau$ | extinction coefficient |
|---|---|---|---|
| 1 | piston | 0.2 | 0.5 |
| 2 | preferential | 0.2 | 0.1 |
| 3 | preferential | 0.05 | 0.5 |
| 4 | preferential | 0.2 | 1 |





HESSD
12, 9393–9436, 2015



**Table 3.** Identifying the differences between simulated $\delta^{18}O$ profiles at station 1 and station 4 (reference, blue curve of Fig. 8): comparison of station 1 (profile 1) with intermediate profiles (here as profile 2) obtained transitioning stepwise from station 1 to station 4, by changing one and only one parameter at a time.

| Profile 1 | | | Profile 2 | | | | |
|---|---|---|---|---|---|---|---|
| Infiltration | ext_c | Vegetation | Infiltration | ext_c | Vegetation | Meaning | |
| piston | 0.5 | tundra | preferential | 1 | flood | Reference curve | |
| piston | 0.5 | tundra | piston | 1 | tundra | Effect of bare soil fraction per PFT | |
| piston | 0.5 | tundra | preferential | 0.5 | tundra | Effect of infiltration | |
| piston | 0.5 | tundra | piston | 0.5 | flood | Effect of vegetation cover | |





HESSD
12, 9393–9436, 2015




**Figure 1.** The territory of Labytnangi with the measurement sites indicated. Image from Google Earth, map data: ©2015 CNES/Astrium, Landsat, ©2015 DigitalGlobe, ©2015 Google.





HESSD
12, 9393–9436, 2015



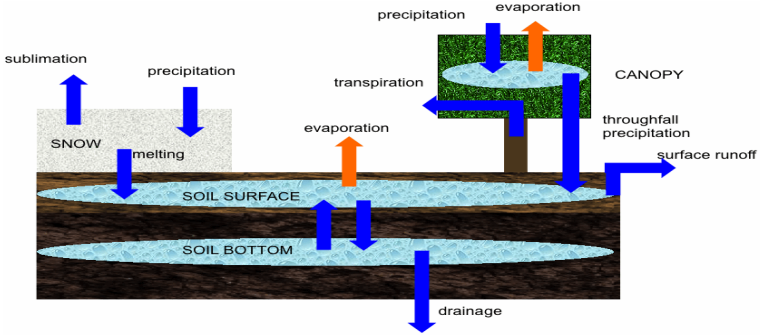


**Figure 2.** A schematic description of ORCHIDEE-iso. In red the processes for which isotopic fractionation occurs.





HESSD
12, 9393–9436, 2015

Simulating hydrology with an isotopic land surface model in western Siberia

F. Guglielmo et al.



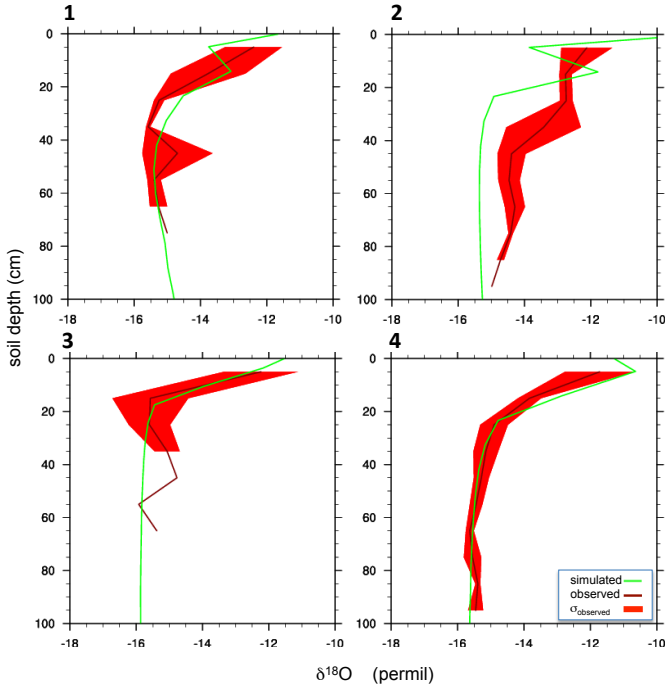


**Figure 3.** $\delta^{18}O$ profiles in soil moisture in situ (brown curves) and from the simulations best fitting the experimental data (green curves, July averages) for the four observation sites. The red area around the experimental curves denotes the standard deviation associated with the spatial variability of the observations (three profiles for each station). Due to the inhomogeneity of the territory, not all profiles reached the same maximum depth. It has been thus possible to estimate the standard deviation only at depths where more than one observed value was available.





HESSD
12, 9393–9436, 2015

Simulating hydrology with an isotopic land surface model in western Siberia

F. Guglielmo et al.



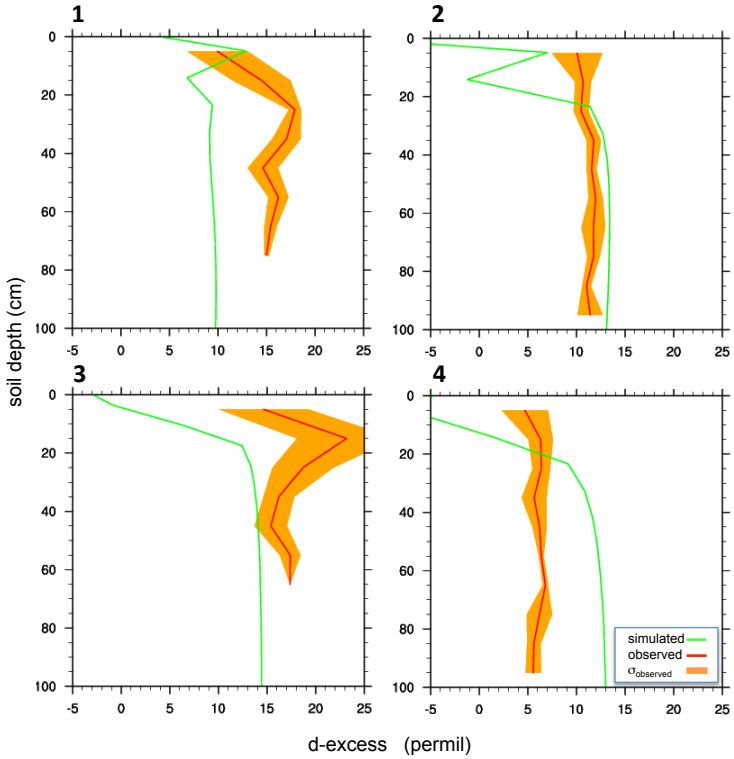


**Figure 4.** d-excess calculated from in situ $\delta$D and $\delta^{18}$O averaged vertical profiles (red curve) and simulated profiles corresponding to the best fitting profiles of Fig. 3 (green curve, July averages). As for $\delta^{18}$O, we show (orange shading around red curves) the standard deviation related to the spatial variability, in this case, of the calculated d-excess profiles. We chose to display and consider this rather than the theoretical error based on the errors of the addends in Eq. (3) in order to take into account possible unknown covariance of $\delta$D and $\delta^{18}$O.





HESSD
12, 9393–9436, 2015

Simulating hydrology with an isotopic land surface model in western Siberia

F. Guglielmo et al.



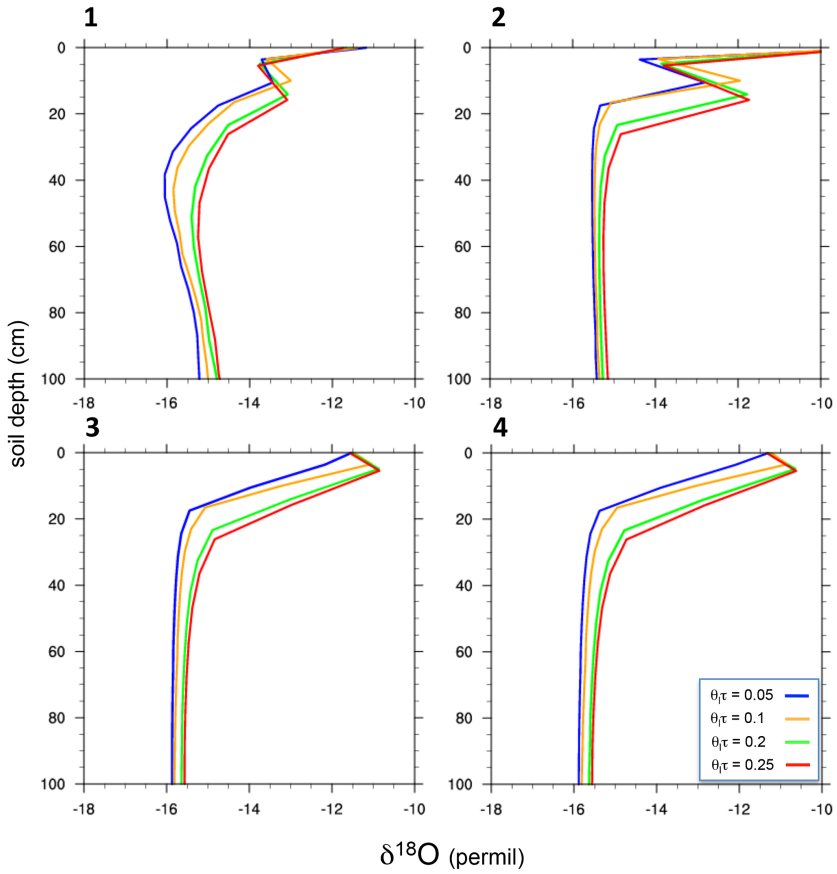


**Figure 5.** Sensitivity of the simulated $\delta^{18}O$ profiles to the vertical diffusivity (July averages). Different colors show different values of the product of the soil tortuosity $\tau$ and of the volumetric content of liquid water $\theta_l$.





HESSD
12, 9393–9436, 2015



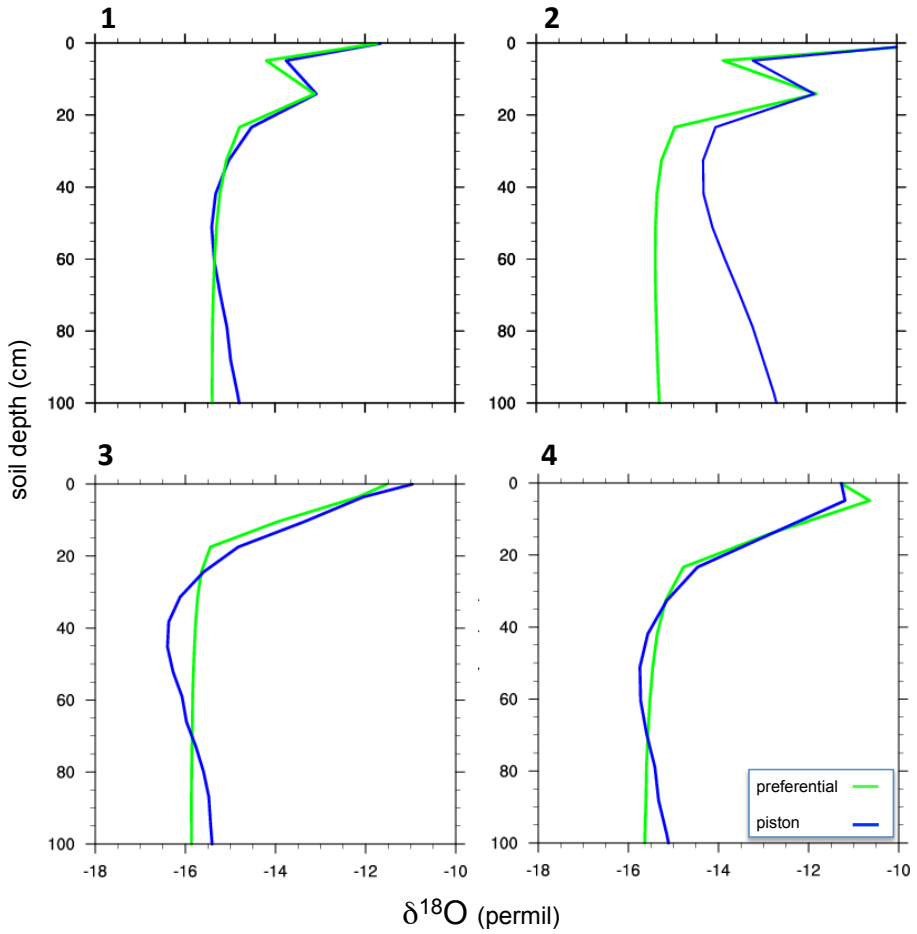


**Figure 6.** Sensitivity of the simulated $\delta^{18}O$ profiles to the infiltration pathway (July averages). Different colors show piston or preferential flow.





HESSD
12, 9393–9436, 2015

Simulating hydrology with an isotopic land surface model in western Siberia

F. Guglielmo et al.



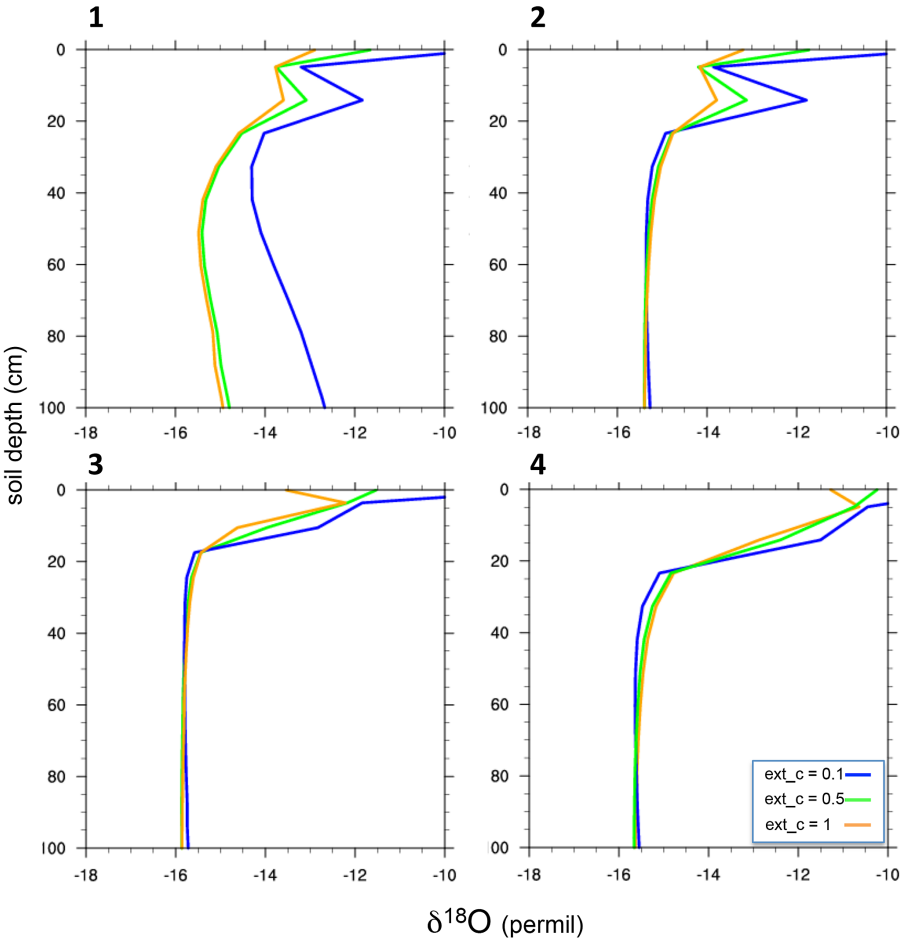


**Figure 7.** Sensitivity of the simulated $\delta^{18}O$ profiles to the bare soil fraction (July averages). Different colors show different values of the extinction coefficient ext_c.





HESSD
12, 9393–9436, 2015

Simulating hydrology with an isotopic land surface model in western Siberia

F. Guglielmo et al.



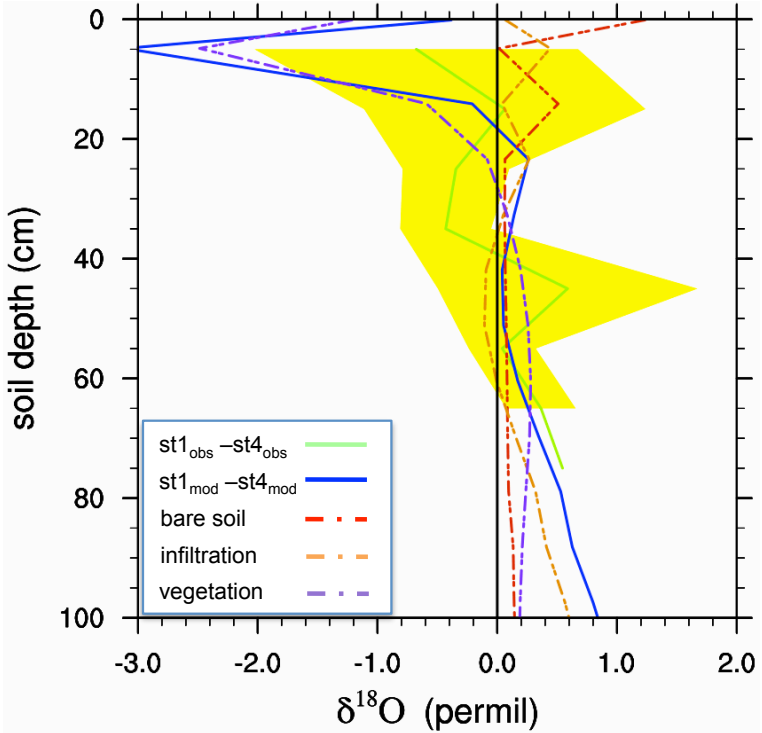


**Figure 8.** Differences between stations 1 (silty tundra) and 4 (floodplain) in terms of observed $\delta^{18}O$ (green curve, with associated error in yellow) and model best fits (blue curve, July averages). The other curves (red, orange, violet) express the transition between the two stations varying one parameter at a time (Table 3).





HESSD
12, 9393–9436, 2015



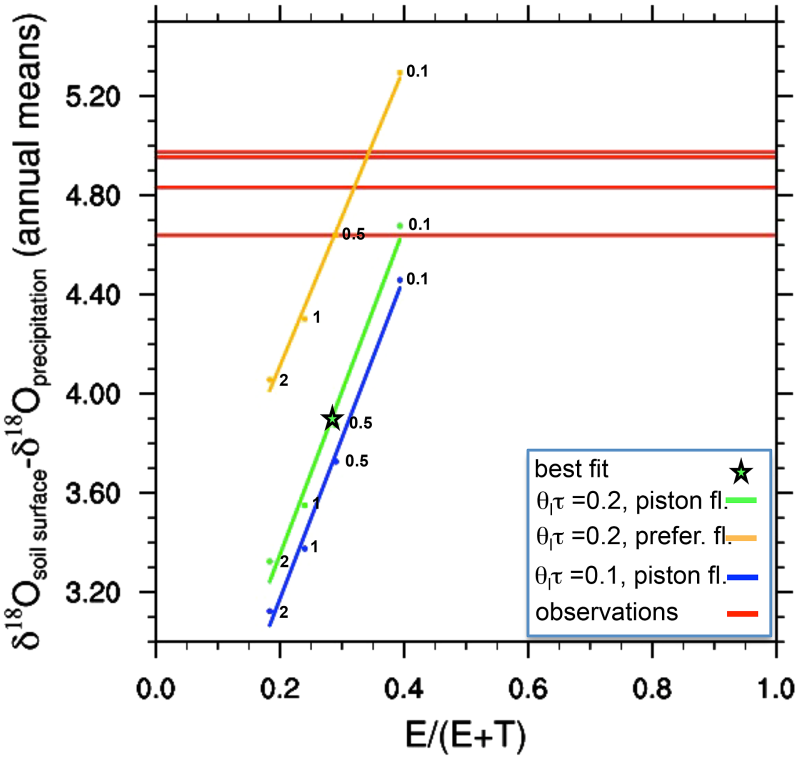






HESSD
12, 9393–9436, 2015

Simulating hydrology with an isotopic land surface model in western Siberia

F. Guglielmo et al.



**Figure 9.** Red lines: difference between $\delta^{18}O$ observed in surface soil water and in annual mean precipitation calculated weighting the monthly mean values by the simulated monthly mean of the difference between precipitation and evapotranspiration (sum of bare soil evaporation and transpiration), at station 1. Different red lines correspond to different $ET$ values obtained with different bare soil fractions in the simulations with ORCHIDEE-iso. Yellow, green and blue points: difference of simulated $\delta^{18}O$ in soil and $\delta^{18}O$ in precipitation vs. simulated $E/(E+T)$ from ORCHIDEE-iso experiments with different bare soil fraction, vertical diffusivity, and infiltration pathway. Each point corresponds to a different model run. The diagonal lines fit points sharing the same $\theta_l\tau$, and infiltration pathway (piston or preferential flow), but having different values (namely 0.1, 0.5, 1, 2) for the light extinction coefficient. The star corresponds to the model best fit of Fig. 3 and the green line fits such point with the other experiments sharing the same $\theta_l\tau = 0.2$ and the piston infiltration pathway. Using this combination as a reference, we vary once at a time the two parameters obtaining, for lower $\theta_l\tau$, the points on the blue line, and, for preferential flow infiltration, the values in orange. The intersection between lines fitting model results and observation lines indicates realistic values of $E/(E+T)$.





HESSD
12, 9393–9436, 2015